J Fluoresc (2011) 21:653–662
DOI 10.1007/s10895-010-0753-7

ORIGINAL PAPER

Rare Earth Centered Hybrid Materials: Tb^{3+} Covalently Bonded with La^{3+}, Gd^{3+}, Y^{3+} Through Sulfonamide Bridge and Luminescence Enhancement

Kai Sheng · Bing Yan · Xiao-Fei Qiao

Received: 5 April 2010 / Accepted: 18 October 2010 / Published online: 30 October 2010

Abstract The organic ligand 5-sulfosalicylic acid (SSA) is grafted by (3-aminopropyl) triethoxysilane (APTES) to achieve functionalized sulfonamide bridge (SSA-Si) which can both coordinate to Ln^{3+} to form luminescent center and link inorganic Si-O network through hydrolysis and condensation reaction with tetraethoxysilane (TEOS). Thus the organic–inorganic hybrid is obtained with sol-gel method. The organic polymer poly-methyl methacrylate (PMMA) acts as another precursor is prepared through the direct addition polymerization of MMA monomer in the presence of the initiator BPO (benzoyl peroxide). The two kinds of precursors are coordinated to the Ln^{3+} simultaneously to form organic–inorganic-polymeric hybrids which contain both inorganic Si-O-Si net and organic periodic C–C chains. In these complicated compounds we intercalate different ratios of Tb^{3+} and inert lanthanide ion (La^{3+}, Gd^{3+}, Y^{3+}) and find that the introduction of the inert lanthanide ions can enhance the luminescence intensity. This enhancement phenomenon is called co-luminescence effect which is studied by emission spectra in this paper.

Keywords Rare earth ion · Organic–inorganic-polymeric hybrids · Energy transfer · Co-luminescence

Introduction

In recent years, hybrid organic–inorganic materials which appear as new multifunctional materials have gained great interest due to their unusual features [1, 2]. The organic–inorganic hybrids combine the organic composite and the inorganic particle within nano scale, which holds excellent physical and chemical properties that pure organic or inorganic phase did not have [3–5]. Among the various approaches, the sol-gel process based on hydrolysis and poly-condensation reactions of metal alkoxides is a convenient method to prepare inorganic–organic hybrid materials with unique properties both in terms of chemical composition and physical microstructure [6–8]. In addition, the mild chemical conditions allowed by the sol-gel process provide a versatile access to form organic–inorganic nanocomposites.

Rare earth complexes have been well known as an important ingredient in luminescent materials for their fascinating properties such as sharp and intense emission bands which is ascribed to the unfilled f-f electronic transitions of lanthanide ions, long radiative lifetimes and potential high internal quantum efficiency [9, 10]. In these systems, organic components can absorb abundant energy under ultraviolet radiation and transferred the energy to lanthanide ions, so called “antenna effect”, and consequently sensitize the lanthanide ions for characteristic luminescence. However, the intrinsic disadvantages such as poor thermal stability and low mechanical strength restrict their applications [8, 11]. Therefore, many researchers have been attracted to the incorporation of small lanthanide complexes into inert matrices to obtain sol-gel derived rare earth organic–inorganic hybrid materials and overcome these shortcomings [6–8, 12–14]. So far, there have been two main classes for rare earth organic–inorganic hybrid materials according to the mutual interaction between organic phase and inorganic host [15]. Class I hybrids are prepared through direct dispersion or dissolution of the rare earth complex into matrix. Although the rare earth complex

K. Sheng · B. Yan (✉) · X.-F. Qiao
Department of Chemistry, Tongji University,
Siping Road 1239,
Shanghai 200092, China
e-mail: byan@tongji.edu.cn

and the matrix can be chosen independently, it is difficult to achieve hybrids with high luminescence intensity and homogeneity of the two phases which is attributed to the weak physical interaction (such as hydrogen bonding, van der Waals force or electrostatic forces) and incompatibility of the two parts [6–9]. While Class II hybrids obtained by linking the two parts with covalent bonds can realize molecular-level complex, thus the leaching or clustering of the emitting center can be avoided, higher concentration of rare earth complexes and homogeneity of the two phases can be obtained [12–14]. As a consequence, many research groups have dedicated to construct molecular based sol-gel derived rare earth organic–inorganic hybrid materials [12–14, 16–24].

Organic–inorganic hybrids doped with rare earth complexes have shown as excellent luminescent materials since the characteristic f-f electronic transition have been studied extensively. Many researchers mainly focused on luminescence of single rare earth ions while few reports have been unfolded for co-luminescence effect of multi rare earth ions [25–27]. When La^{3+}, Gd^{3+}, Lu^{3+}, Y^{3+} are incorporated with Eu^{3+} or Tb^{3+} at appropriate molar ratio, a luminescence enhancement phenomenon is found and they also found that all the enhancing ions have a stable electronic configuration such as La^{3+}, Y^{3+}, Gd^{3+} and Lu^{3+}, the 4f shells of which are empty, half-filled and full, respectively [25–27]. In this paper, we not only incorporate these inert rare earth ions into Tb^{3+} organic–inorganic hybrids but also immobilize organic polymer in the hybrid system (named organic–inorganic-polymeric hybrids). The organic polymer PMMA possessing attractive properties such as transparency, lightweight, are easily to be fabricated and conveniently to be controlled various optical parameters, and it is proved that the higher luminescence intensity and more regular morphology of the resulting material we obtained [28–31]. Here, we synthesize a series of molecular based rare earth organic–inorganic hybrids and rare earth organic–inorganic polymeric hybrids with different ratios of inert rare earth ions and active rare earth ions (Tb^{3+}). The results reveal that the organic–inorganic-polymeric hybrids exhibit higher emission intensity, and the co-existence of inert rare earth ions can make the luminescence better.

Experimental

Chemicals

Terbium nitrate is obtained by dissolving corresponding oxides in concentrated nitric acid. 5-sulfosalicylic acid (SSA) is provided by Lancaster Synthesis Ltd. 3-aminopropyltriethoxysilane (APTES) is supported by Alfa Company. The tetraethoxysilane (TEOS) is supplied by Aldrich. Methyl methacrylate (MMA) is purchased from Shanghai chemical plant. The common solvents are purchased from China National Medicine Group (A.P.). Other starting reagents are used as received.

Synthesis of the Precursor SSA-Si

One mmol SSA is first dissolved in refluxing anhydrous tetrahydrofuran (THF) by stirring, and then 0.5 mmol thionyl chloride is added to the solution by drops. The whole mixture is refluxing at 120 °C for 3 h under argon in a covered flask. Then 1 mmol APTES is added in the solution and are refluxing at 80 °C for 6 h. After cooling, the solvent is removed using a rotary vacuum evaporator, and then the residual is ished with 20 ml of hexane three times. A yellow oil is obtained (see Scheme 1). Yield: 75 %. *Anal. Calcd.* for $C_{16}H_{27}O_8NSSi$ (%): C 45.59, H 6.46, N 3.32; Found: C 44.53, H 6.17, N 3.26. ^1H NMR ($CDCl_3$, 400 MHz): δ 0.53(t, 2H, CH_2Si), 1.38(t, 9H, CH_3), 1.62(m, 2H, $CH_2CH_2CH_2$), 3.26(m, 2H, $NHCH_2$), 3.86 (q, 6H, $SiOCH_2$), 7.39(d, 1H,$-C_6H_4$), 7.56(d, 1H,$-C_6H_4$), 7.95(t, 1H, *NH*), 8.32(d, 1H,$-C_6H_4$), 11.78(s, 1H, *OH*), 12.10 (s, 1H, *COOH*).

Synthesis of Organic Polymer PMMA

One mmol Methyl methacrylate is weighed and transferred into separating funnel, and then it ished with 0.1 mol/L sodium hydroxide solutions to remove the inhibitor. After oscillating for 5 min and standing for 2 h, separation of the water phase and upper oil phase is carried on. The residual water is removed with anhydrous copper sulfate. After purification and reduced pressure distillation under nitrogen atmosphere, the monomer is injected into covered three mouth flask with benzoyl peroxide BPO as an initiator. The mixture is dissolved in blend-solvent (BS) of toluene and ethyl acetate and maintained at 70 °C for 8 h under flowing high purity nitrogen. After removing of the solvent, a canary yellow and stringy liquid is obtained. The product is dried in vacuum desiccator after recrystallization using methanol and anhydrous ether.

Synthesis of the Organic–Inorganic Hybrids with Si-O Networks

SSA-Si is dissolved in DMF (dimethylformamide). Then a stoichiometric amount of $Tb(NO_3)_3{\cdot}6H_2O$ (1 mmol/L, EtOH) is added to the solution with stirring drop by drop. After 2 h, a stoichiometric amount of tetraethoxysilane (TEOS) and one drop of diluted hydrochloric acid are put into the solution to promote hydrolysis. The molar ratio of $Tb(NO_3)_3{\cdot}6H_2O$/SSA-Si/TEOS/H_2O is 1: 3: 6: 24. Then we get the hybrid material after removing the solvent at 80 °C in 5 days (see Scheme 1).

Scheme 1 The synthesis route of the precursor SSA-Si (I), the predicted structure of the organic–inorganic hybrids (II) and the organic–inorganic-polymeric hybrids (III)

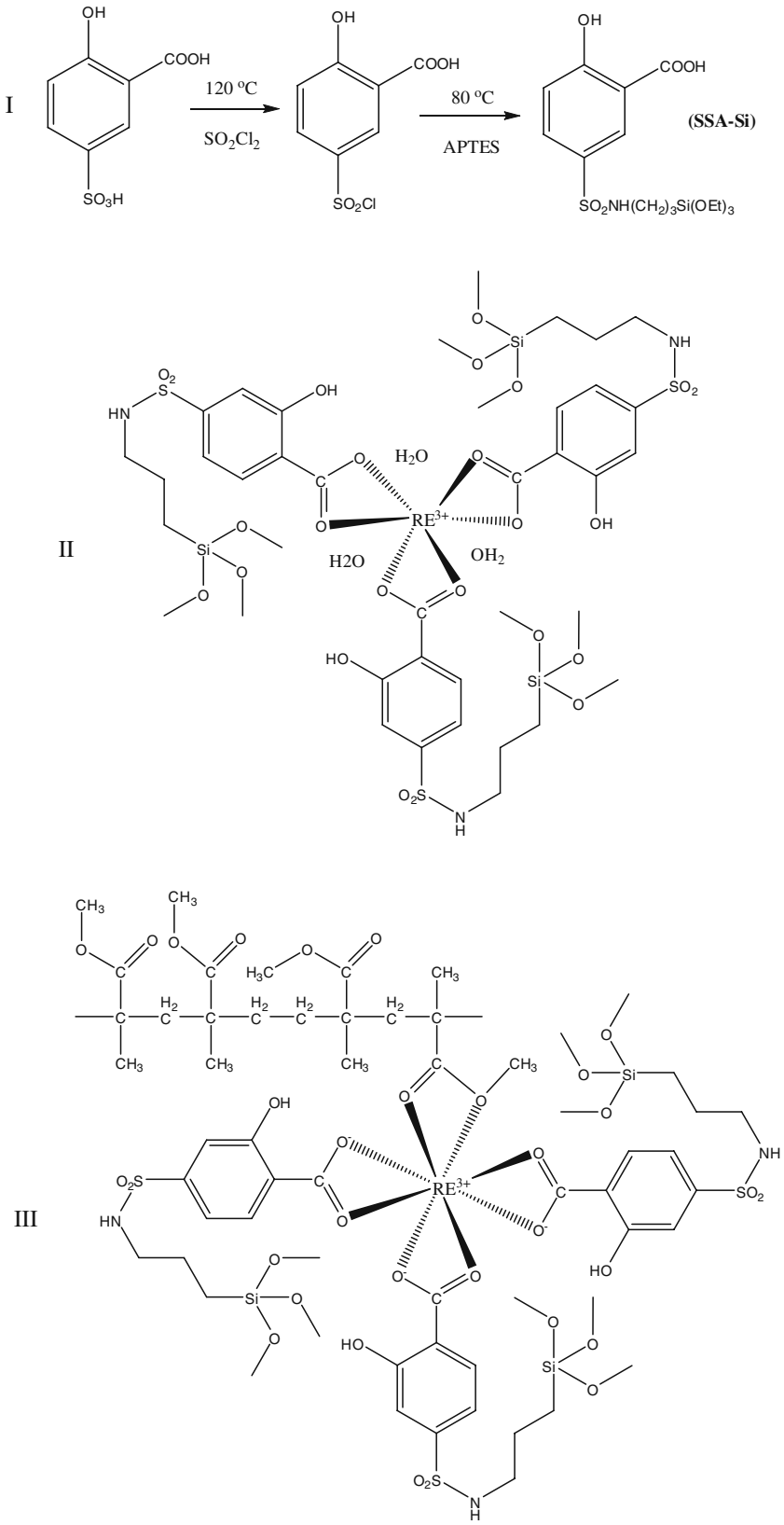

Synthesis of the Organic–Inorganic-Polymeric Hybrids

Similar to the method above: SSA-Si and the organic polymer PMMA are dissolved in DMF simultaneously and then Tb $(NO_3)_3{\cdot}6H_2O$ is added . Then a stoichiometric amount of TEOS and HCl is put into the solution. The mole ratio of Tb $(NO_3)_3{\cdot}6H_2O$/SSA-Si/MMA/TEOS/H_2O is 1: 3: 1: 6: 24. After gelation in an oven at 80 °C in a few days we obtained the hybrids containing not only inorganic Si-O networks but also organic C–C chains (see Schemes 1 and 2).

Using the same method, we prepared the Tb^{3+} and inert lanthanide ions (La^{3+}, Gd^{3+}, Y^{3+}) co-hybrid materials with and without polymer by mixing Tb^{3+} and inert ions at different ratios. These hybrids are named Tb-Gd31, Tb-Gd21, Tb-Gd11, Tb-Gd12, Tb-Gd13, PM-Tb-La31, PM-Tb-La21 and so on (here the number means the molar ratio of Tb to Gd, i.e. Tb-Gd31 referes to Tb: Gd = 3: 1) (see Schemes 1 and 2).

Physical Characterization

All measurements are performed at room temperature. Infrared spectra are recorded on a Nexus 912 AO439 FT-IR spectrophotometer. We mixed the compound with the dried potassium bromide (KBr) and then pressed into pellets. The spectra are collected over the range 4000–400 cm^{-1} by averaging 32 scans at a maximum resolution of 8 cm^{-1}. ^1H NMR spectra are recorded in $CDCl_3$ on a Bruker AVANCE-400 spectrometer with tetramethylsilane (TMS) as an internal reference. The ultraviolet-visible diffuse reflection spectra of the powder samples are recorded by a BWS003 spectrophotometer. X-ray powder diffraction patterns are recorded using a Rigaku D/max-rB diffractometer system equipped with a Cu anode in a 2θ range from 10° to 70°. The luminescence spectra are obtained on a RF-5301 spectrophotometer equipped with a stablespec-xenon lamp (450 W) as the light source. The microstructures are checked by scanning electronic microscopy (SEM, Philip XL-30).

Results and Discussion

APTES Functionalized Molecular Precursor SSA-Si

Figure 1a shows the Fourier transform infrared spectra of the free ligand SSA (A) and the precursor SSA-Si (B). It

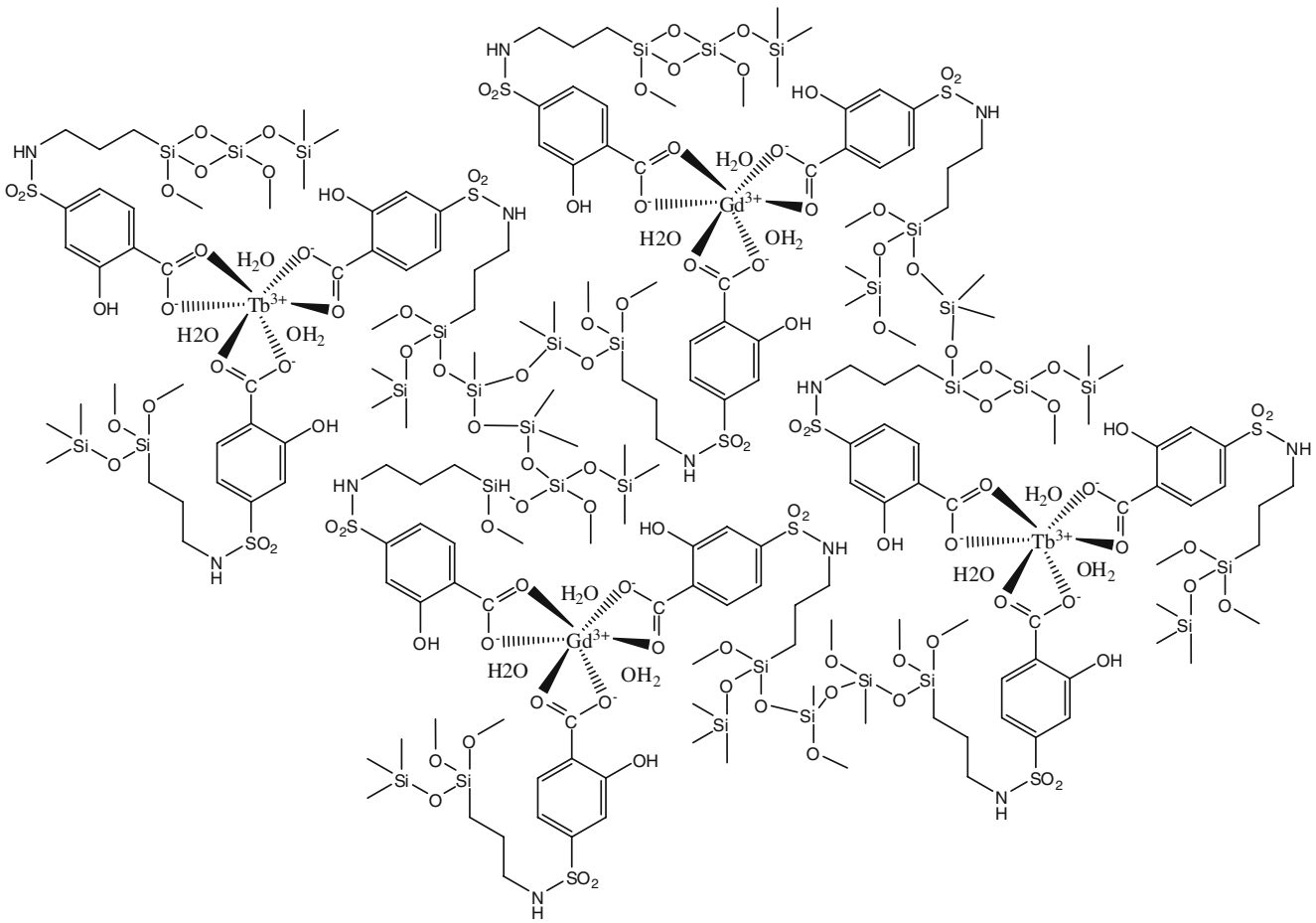

Scheme 2 The predicted structure of the co-doped Tb-Gd hybrids

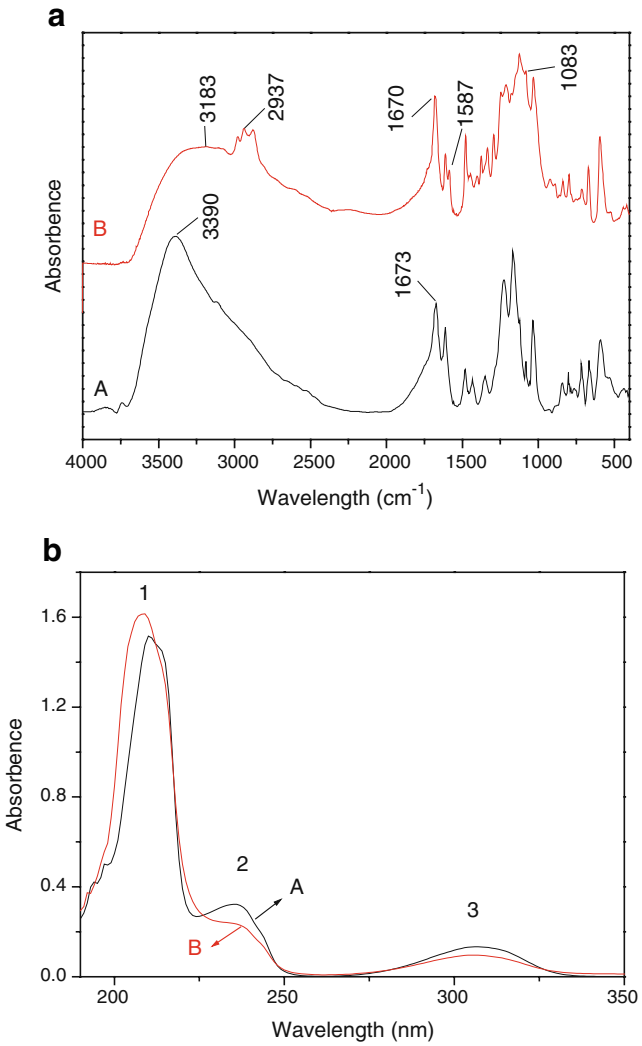

Fig. 1 The Fourier transform infrared spectra (**a**) and the ultraviolet absorption spectra (**b**) of the free ligand SSA (*A*) and the precursor SSA-Si (*B*)

can be seen from Fig. 1a, there is a strong band centered at 3,390 cm^{-1} which is ascribed to the stretching vibration of −OH. And this absorption is taken place by a broad scattered band centered at about 3,183 cm^{-1} in Fig. 1b, which indicates the hydroxyl groups become associated and consequently result in the weak absorption of N-H stretching vibration is covered. The peaks at 1,673 cm^{-1} and 1,670 cm^{-1} in Fig. 1a and b are corresponded to stretching vibration of C = O. The three continuous peaks at about 2,937 cm^{-1} which is originated from the three methylene groups of APTES and the new peak appeared at 1,587 cm^{-1} which derives from the in-plain bending vibration of N-H confirm that the silane coupling reagent 3-aminopropyltriethoxysilane is successfully grafted onto organic free ligand SSA. Furthermore, the asymmetric stretching vibration of Si-O is evidenced by the peak locating at 1,083 cm^{-1}.

Figure 1b shows the ultraviolet absorption spectra of the free ligand SSA (A) and the precursor SSA-Si (B). From the curve, we can see three bands (marked 1, 2, 3) which locates at 207, 235 and 306 nm for A (for B, they are 210, 235 and 306 nm) in both spectra. The strongest absorption peak 1 is due to the π–π* electronic transition and the peaks 2 and 3 are ascribed to the superposition of the electronic cloud. Comparing the absorption spectrum of SSA-Si (B) with that of SSA (A), we can see a small blue-shift of the major π–π^* electronic transitions (from 210 to 207 nm) which indicate that the modification of SSA result in the change of the whole electronic conjugating system.

Silica Based Hybrid Materials

Figure 2 presents the X-ray diffraction (from 10 to 70°) spectra of the selected hybrid materials: Tb hybrids (A), Tb-La11 hybrids (B), PM-Tb-La11 hybrids (C), which reveals that all the obtained hybrid materials are amorphous in the whole range. All the materials exhibit the similar XRD patterns with a broad peak centered at around 23° which is the characteristic diffraction of amorphous siliceous backbone material [32–34]. By comparison with the three hybrids, there is no new diffraction peaks for the pure rare earth complex or PMMA show that the introduction of the macromolecular ligands in the hybrid system did not bring changes on the disordered silicon skeleton but make the overall system more disordered. Furthermore, there are many narrow weak peaks in these samples which correspond to the incomplete hydrolysis-condensation of the excessive TEOS molecules. TEOS molecules can carry on hydrolysis-condensation process themselves or with silane coupling reagent. If the hydrolysis-condensation process of

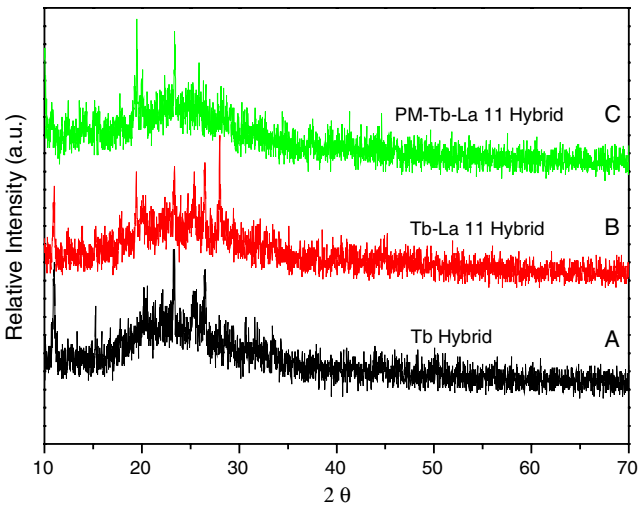

Fig. 2 The X-ray diffraction spectra of the selected hybrid materials (*A* denotes Tb hybrids, *B* denotes Tb-La11 hybrids and *C* denotes PM-Tb-La 11 hybrids)

the excessive TEOS molecular takes place among themselves, the ordered Si-O network can form a better crystal state. Then the narrow peaks appear. But the small amount of the ordered Si-O network brings the weak intensity. In addition, neither of the sample exhibit the measurable amounts of the phase corresponding to the free ligands or the free salts which can support that the formation of the covalently bonded hybrids.

Figure 3 exhibits the ultraviolet-visible diffuse reflection absorption spectra of the selected hybrid materials: Tb hybrids (A), Tb-La11 hybrids (B), Tb-Gd11 hybrids (C), Tb-Y11 hybrids (D). As can be seen obviously in Fig. 3, there is a large broad absorption band in each hybrids which is attributed to the π–π* electronic transition of the aromatic ring in the hybrid system. It is worth noting that the large broad band overlaps (from 240 to 500 nm) with the excitation spectra (from 270 to 350 nm). These energy can be transferred to lanthanide ions through "antenna effect" and sensitize the lanthanide ions. Furthermore, there exist some obvious inverse peaks in each hybrids, at 489, 545, 586 and 623 nm, respectively, which are corresponding to the characteristic emission of terbium ions (Fig. 4). The intensity of the Tb-Gd11 Hybrids is the highest and there exists splitting phenomena on the main inverse peak at 545 nm which is also in accord with the emission spectra of the hybrids (see Fig. 4).

Photoluminescence Properties

To investigate the co-luminescence effect caused by the interaction between inert rare earth ions and active rare earth ions, we firstly incorporate different inert ions La^{3+}, Gd^{3+}, Y^{3+} in Tb^{3+} organic–inorganic hybrid system with the same ratio 1 : 1. As shown in Fig. 4, the excitation and emission spectra

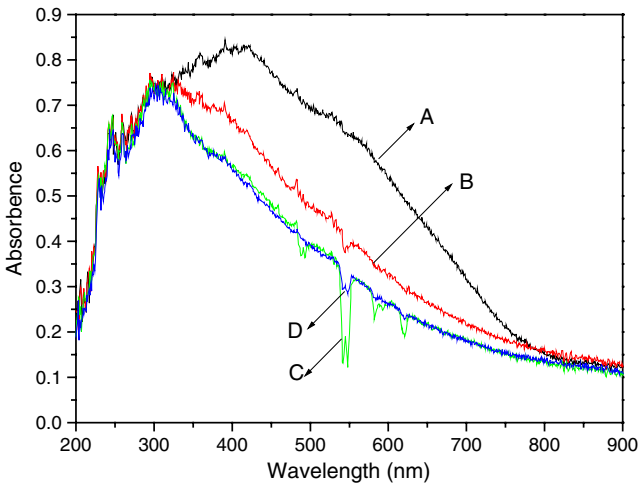

Fig. 3 The ultraviolet-visible diffuse reflection absorption spectra of the selected hybrid polymeric materials: Tb hybrids (*A*), Tb-La11 hybrids (*B*), Tb-Gd11 hybrids (*C*), Tb-Y11 hybrids (*D*), respectively

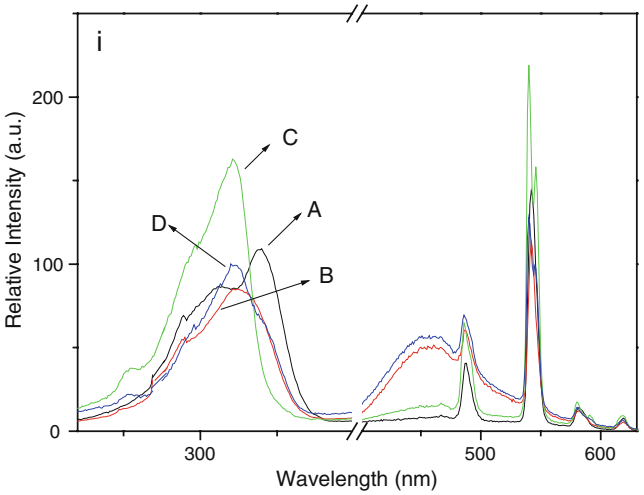

Fig. 4 The luminescent excitation and emission spectra of the hybrid materials (*A* represents Tb hybrids, *B* represents Tb-La11, *C* represents Tb-Gd11 and *D* represents Tb-Y11, respectively)

of these organic–inorganic hybrids are measured on solid powders at room temperature. All the excitation spectra which is obtained by monitoring the maximum emission line of terbium ion ($^5D_4$-$^7F_5$) exhibit a broad band in the range of 270–350 nm (mentioned above) which is assigned to the transition of the organic ligand from the ground state S_0 to the excited state S_1 [35–37]. Moreover, the blue-shift of the maximum excitation wavelength comparing the hybrids Tb-La11 (B), Tb-Gd11 (C), Tb-Y11 (D) with the Tb hybrids (A) demonstrate that the environment surrounding Tb^{3+} has been changed with the introduction of the rare earth inert ions. The emission spectra of the hybrid materials in Fig. 4 are obtained by monitoring the optimal excitation wavelength 320 nm for B, C and D, while 340 nm for A. It can be observed that all the hybrids exhibit characteristic Tb^{3+} cation emission lines 486, 542, 581 and 618 nm corresponding to $^5D_4 \rightarrow {}^7F_J$ (J=6-3) transition. In addition, the dominant $^5D_4 \rightarrow {}^7F_2$ green emission intensity (arbitrary units / a.u.) of the Tb-Gd11 hybrids is stronger than other hybrids which suggest that the co-luminescence effect brought by interaction of inert ions Gd^{3+} and active ions Tb^{3+} occur. The luminescence intensity of Tb-Gd11 (a.u., 219.1) is more than 1.5 times than Tb hybrid (a.u., 143.9). The mechanism of this co-luminescence enhancement effect will be explained later.

For the sake of finding a best ratio between Tb^{3+} and Gd^{3+} for luminescence in this molecular based organic–inorganic hybrid system, we further prepare Tb-Gd31 (A), Tb-Gd21 (B), Tb-Gd11 (C), Tb-Gd12 (D), Tb-Gd13 (E), and Tb hybrids (F) as shown in Fig. 5. The results show that all the Tb-Gd co-exist hybrids exhibit higher intensity than hybrid system containing Tb^{3+} only for both excitation and emission spectra. Meanwhile, for the co-exist hybrid system all the excitation peaks shift from 340 to 320 nm

and each of the characteristic emission peak split into double peaks. From the point of view above, we can come to a conclusion that the SSA chelated terbium hybrids exhibit good luminescence characteristics and this is much enhanced when the inert ions Gd^{3+} is incorporated into this Tb^{3+} hybrid system in molecular level. Comparing with Tb-Gd co-doped system from Fig. 5, for A, B and E, the excitation and emission lines are overlapped and Tb-Gd 12 hybrids exhibit strongest intensity (a.u., 507.9 more than 3.5 times comparing with Tb hybrid) than others in the silica based organic–inorganic system. The luminescence intensity do not increase along with the increasing concentration of Tb^{3+} in the co-doped system which can also sustain the fact that co-luminescence effect arise.

Because the organic polymer such as PMMA, PVPD (poly-vinylpyridine) and PMAA (poly-methacrylic acid) can facilitate the luminescence properties in sol-gel derived hybrids through replacement of coordinated water molecular and efficient energy transfer [30, 31, 38], we prepare co-doped organic–inorganic-polymeric hybrids containing polymer PMMA through incorporating inert ions La^{3+}, Gd^{3+}, Y^{3+} in Tb^{3+} hybrid system. The excitation and emission spectra of these hybrids are shown in Fig. 6. They are PM-Tb (A), PM-Tb-La11 (B), PM-Tb-Gd11 (C), PM-Tb-Y11 (D), respectively. The relative intensity of the organic–inorganic-polymeric hybrids increases according to the sequence D < A < C < B, and the emission intensities of B (a.u., 677.0) are much stronger than those of A (a.u., 209.2) and C (a.u., 302.5). Corresponding to the excitation spectrum, the luminescent intensities of hybrids changed with the same sequence. Moreover, comparing to the Tb hybrid without polymer, the luminescence intensity of PM-Tb hybrid (a.u., 209.2) is much enhanced indicating the efficient energy transfer from organic polymer PMMA to Tb^{3+} ions.

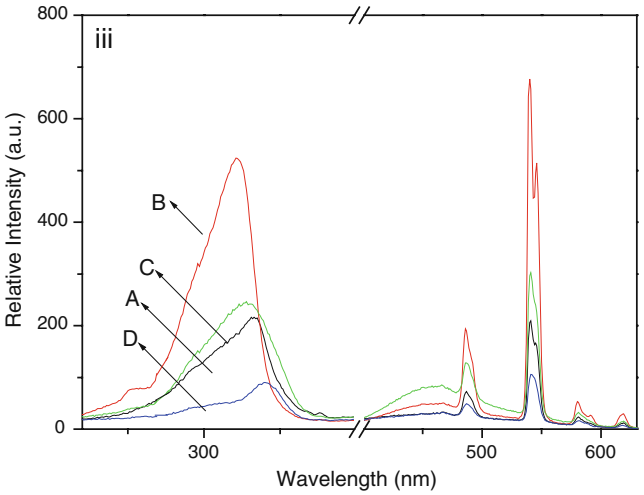

Fig. 6 The luminescent excitation and emission spectra of the hybrid materials (*A* represents PM-Tb hybrids, *B* represents PM-Tb-La11, *C* represents PM-Tb-Gd11 and *D* represents PM-Tb-Y11, respectively)

Similarly, for the sake of finding a best ratio between Tb^{3+} and La^{3+} in this molecular based organic–inorganic-polymeric hybrid system, we further prepare PM-Tb-La31 (A), PM-Tb-La21 (B), PM-Tb-La11 (C), PM-Tb-La12 (D), PM-Tb-La13 (E), and PM-Tb hybrids (F) as shown in Fig. 7. The relative luminescence intensity of the Tb-La co-doped organic–inorganic-polymeric hybrids increases according to the sequence E (a.u., 82.7) < D (a.u., 163.9) < F (a.u., 209.2) < C (a.u., 677.0) < B (a.u., 773.2) < A (a.u., 1052.3), that is, the increase of luminescence intensity alters along with the concentration of Tb^{3+} except F. This result shows that there exist energy transfer from organic

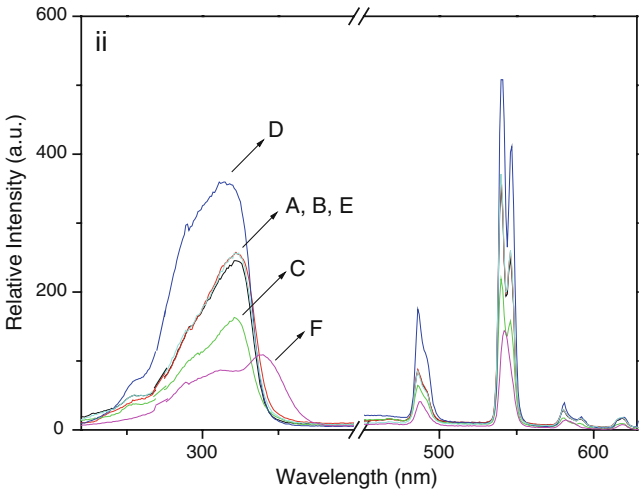

Fig. 5 The luminescent excitation and emission spectra of the hybrid materials (*A* represents Tb-Gd31, *B* represents Tb-Gd21, *C* represents Tb-Gd11, *D* represents Tb-Gd12, *E* represents Tb-Gd13 and *F* represents Tb hybrids, respectively)

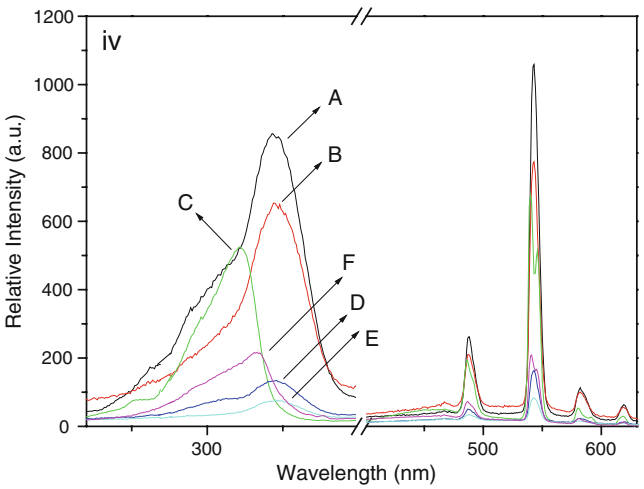

Fig. 7 The luminescent excitation and emission spectra of the hybrid materials (*A* represents PM-Tb-La31, *B* represents PM-Tb-La21, *C* represents PM-Tb-La11, *D* represents PM-Tb-La12, *E* represents PM-Tb-La13 and *F* represents PM-Tb hybrids, respectively)

polymer PMMA to active Tb^{3+} and when Tb^{3+} contents become bigger in some extent the Tb-La co-doped organic–inorganic-polymeric hybrid system exhibit higher luminescence intensity.

Luminescence and Co-luminescence Mechanism

The luminescence behavior is mainly caused by the formation of luminescent center: SSA chelated with active Tb^{3+}. SSA which is considered as excellent ligand possesses versatile coordination modes and can well sensitize lanthanide luminescence [39]. As we know, there are two main steps in the luminescence process: energy transfer from ligand to lanthanide center and reverse energy transition caused by thermal deactivation [40–42]. The energy transfer efficiency is dependent on the intrinsic energy difference (ΔE (T_r–Ln^{3+})) between the lowest triplet state level of ligands and the resonant energy level of the central Ln^{3+}. Nevertheless, we can decrease the non-radiation thermal deactivation mainly caused by hydroxyl vibration of water molecule around Ln^{3+}. Thus, the luminescent center is introduced to the Si-O network via sol-gel method and organic polymer (PMMA for example) which can coordinate to Ln^{3+} is proved to improve the luminescence intensity through replacement of coordinated water molecule.

It is clear that Gd^{3+} has a stable half-filled electronic configuration and it is hard for f-f transition. La^{3+} is impossible for f-f transition since it does not have 4f electrons. Therefore, gadolinium and lanthanum compound can not luminance. Whereas, when these inert lanthanide ions are mixed with the active Tb^{3+} together and then are added to silica based molecular hybrid system at appropriate ratio we found that the emission intensity of the co-doped system is much enhanced. It is considered that the Tb^{3+} and inert ions coexist in the sol-gel derived hybrid systems at molecular level through the process of hydrolysis and poly-condensation. Because both the Tb^{3+} and the inert ions are chelated by SSA-Si which is chemically bonded to the inorganic Si-O network and the distance between Tb^{3+} and inert ion make the intramolecular energy transfer from inert center to active center possible. Furthermore, the active luminescent center is surrounded by the inert part, which make the quencher of ion–ion interaction of Tb^{3+} itself impossible. Besides, the surrounding inert part of active center can form a cage which can not only prevent energy loss but also protect the luminescent center from colliding with water molecules. Therefore, the luminescence intensity is much enhanced in the presence of the inert ions.

However, in organic–inorganic hybrid system the Tb-Gd co-existed system shows the strongest luminescence intensity while in organic–inorganic-polymeric hybrid system the Tb-La co-exist system exhibit strongest luminescence. Such difference can be considered in the following way. In organic–inorganic hybrid system, Tb-SSA-Si complex and Gd-SSA-Si complex is connected by the Si-O network. Because of the best energy matches between the excited energy level of Gd-SSA-Si complex and the resonance energy

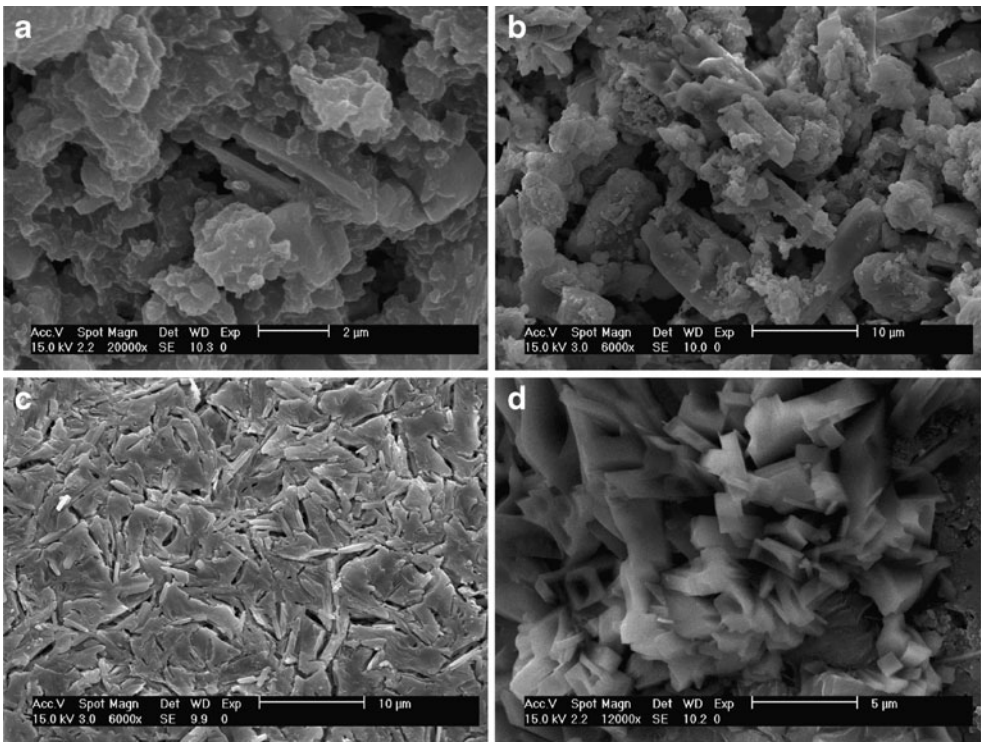

Fig. 8 The scanning electronic micrograph of the selected hybrid materials (*A* for binary Tb hybrids, *B* for Tb-Gd 11, *C* for ternary PM-Tb hybrids and *D* for PM-Tb-La 11, respectively)

level of the triplet states of Tb-SSA-Si complex, the Gd-SSA-Si complex act as an energy-insulating sheath and transferred the absorped energy through covalent Si-O bond to the Tb-SSA-Si complex for radiation. After the introduction of the organic polymer PMMA, both Tb^{3+} ions and inert ions can not only chelate with SSA-Si but also coordinate to the long organic C–C chains of PMMA (Scheme 1 III). The organic polymer PMMA can not only promote adsorption but also change the conformation of the hybrid system, resulting in the difference of energy levels between the Tb^{3+} complex and inert ions complex. Besides, the distances between the Tb^{3+} complex and inert ions complex is closer by PMMA. For the exact different mechanism between organic–inorgic and organic–inorganic-polymeric system, the continuous study is necessary in order to thoroughly understand the energy transfer process.

Microstructure of the Hybrids

The microstructure of the selected hybrid materials are shown in Fig. 8 (A for binary Tb hybrids, B for Tb-Gd 11, C for ternary PM-Tb hybrids and D for PM-Tb-La 11). From all the images, we can see the obvious distinction between the binary and the ternary hybrid materials. For both kinds of hybrids, the phase separation phenomena do not take place in the whole experimental process because the precursor SSA-Si acts as a functional molecular bridge linking the inorganic and organic component by covalent bonds. The ternary hybrid materials exhibit the uniform, regular and ordered microstructure with the dendritic stripe on the surface, which indicate that the self-assemble process occurred with the introduction of the polymer.

Such microstructure of both kinds of hybrid materials can be explained in the following way. For the binary hybrids, the lanthanide ions are chelated to the precursor SSA-Si at the beginning to form the luminescent center. Then the hydrolysis and condensation process appears to be predominant when the TEOS is added in. This process occurred and terminated randomly among SSA-Si itself or between SSA-Si and TEOS within sol-gel mechanism. Because of the rigidity of the luminescent center is weak and easily be affected by ambient Si-O networks, which result in the stochastic, unfixed and indefinite surface morphology. However, for the ternary hybrid materials, the generation of the luminescent center took place among lanthanide ions, SSA-Si and PMMA. The two kinds of precursors coordinated to lanthanide ions simultaneously. Thus, not only the rigidity of the compound is increased but also the periodic organic polymer played a role as a template that the extended order of the macromolecular chain or network could provide a new sort of organization to hydrolysis and condensation process along the polymer backbone, which lead to the ordered microstructure.

Conclusions

A series of silica based molecular hybrids incorporating different inert lanthanide ions (La^{3+}, Gd^{3+}, Y^{3+}) into active Tb^{3+} with different ratio are prepared as transparent monoliths by sol-gel process. All the samples are totally amorphous and exhibit strong luminescence intensity. Moreover, the selected ternary hybrids with long organic C–C chains show more regular microstructure than the bianry hybrids. Besides, in organic–inorganic hybrid system Tb-Gd coexist hybrids exhibit the strongest luminescence intensity while in organic–inorganic-polymeric hybrid system the Tb-La coexist hybrids exhibit the highest luminescence. When the inert ions incorporating within appropriate ratio the luminescence enhancement (so called "co-luminescence effect") take place and this phenomenon is discussed in detail.

Acknowledgements This work is supported by the National Natural Science Foundation of China (20971100) and Program for New Century Excellent Talents in University (NCET-08-0398).

References

1. Naka K, Itoh H, Tampo Y, Chujo Y (2002) Self-organization of spherical aggregates of palladium nanoparticles with a cubic silsesquioxane. Nano Lett 2:1183
2. Kim KM, Keum DK, Chujo Y (2003) Organic–inorganic polymer hybrids using polyoxazoline initiated by functionalized silsesquioxane. Macromolecules 36:867
3. Kurmoo M (1999) Ferrimagnetism in dicarboxylate-bridged cobalt hydroxide layers. J Mater Chem 10:595
4. Gómez-Romero P, Chojak M, Cuentas-Gallegos K, Asensio JA, Kulesza PJ, Casañ-Pastor N, Lira-Cantú M (2003) Hybrid organic–inorganic nanocomposite materials for application in solid state electrochemical supercapacitors. Electrochem Commun 5:149
5. Zhang ZJ, Xiang SC, Zhang YF, Wu AQ, Cai LZ, Guo GC, Huang JS (2006) A new type of hybrid magnetic semiconductor based upon polymeric iodoplumbate and metal-organic complexes as templates. Inorg Chem 45:1972
6. Matthews LR, Knobbe ET (1993) Luminescence behavior of europium complexes in sol-gel derived host materials. Chem Mater 5:1697
7. Sanchez C, Ribot F, Rozes L, Alonso B (2000) Design of hybrid organic–inorganic nanocomposites synthesized via sol-gel chemistry. Mol Cryst Liq Cryst 354:143
8. Menaa B, Takahashi M, Tokuda Y, Yoko T (2007) Preparation and properties of polyphenylsiloxane-based hybrid glass films obtained from a non-aqueous coating sol via a single-step dip-coating. Opt Mater 29:806
9. Gunnlaugsson T, Leonard JP (2003) H^+, Na^+ and K^+ modulated lanthanide luminescent switching of Tb(III) based cyclen aromatic diaza-crown ether conjugates in water. Chem Commun 19:2424
10. Quici S, Cavazzini M, Marzanni G, Accorsi G, Armaroli N, Ventura B, Barigelletti F (2005) Visible and near-infrared intense luminescence from water-soluble lanthanide [Tb(III), Eu(III), Sm (III), Dy(III), Pr(III), Ho(III), Yb(III), Nd(III), Er(III)] complexes. Inorg Chem 44:529

11. Tanner PA, Yan B, Zhang HJ (2000) Preparation and luminescence properties of sol-gel hybrid materials incorporated with europium complexes. J Mater Sci 35:4325
12. Escribano P, Julián-López B, Planelles-Aragó J, Cordoncillo E, Viana B, Sanchez C (2008) Photonic and nanobiophotonic properties of luminescent lanthanide-doped hybrid organic–inorganic materials. J Mater Chem 18:23
13. Binnemans K (2009) Lanthanide-based luminescent hybrid materials. Chem Rev 109:4283
14. Lenaerts P, Storms A, Mullens J, Haen JD, Göller-Walrand C, Binnemans K, Driesen K (2005) Thin films of highly luminescent lanthanide complexes covalently linked to an organic–inorganic hybrid material via 2-substituted imidazo[4, 5-f]-1, 10-phenanthroline groups. Chem Mater 17:5194
15. Sanchez C, Ribot F (1994) Design of hybrid organic–inorganic materials synthesized via sol-gel chemistry. New J Chem 18:1007
16. Carlos LD, Ferreira RAS, Bermudez VD, Ribeiro JLS (2009) Lanthanide-containing light-emitting organic–inorganic hybrids: a bet on the future. Adv Mater 21:509
17. Lunstroot K, Driesen K, Nockemann P, Göller-Walrand C, Binnemans K, Bellayer S, Bideau JL, Vioux A (2006) Luminescent ionogels based on europium-doped ionic liquids confined within silica-derived networks. Chem Mater 18:5711
18. Sanchez C, Julian B, Belleville P, Popall M (2005) Applications of hybrid organic–inorganic nanocomposites. J Mater Chem 15:3559
19. Minoofar PN, Hernandez R, Chia S, Dunn B, Zink JI, Franville AC (2002) Placement and characterization of pairs of luminescent molecules in spatially separated regions of nanostructured thin films. J Am Chem Soc 124:14388
20. Choi J, Tamaki R, Kim SG, Laine RM (2003) Organic/inorganic imide nanocomposites from aminophenylsilsesquioxanes. Chem Mater 15:3365
21. Lima PP, Ferreira RAS, Freire RO, Almeida Paz FA, Fu LS, Alves S Jr, Carlos LD, Malta OL (2006) Spectroscopic study of a UV-photostable organic–inorganic hybrids incorporating Eu^{3+} β-diketonate complex. ChemPhyChem 7:735
22. Yan B, Wang QM (2008) First two luminescent molecular hybrids composed of bridged Eu(III) β−diketone chelates covalently trapped in silica and titanate gels. Cryst Growth Des 6:484
23. Yan B, Lu HF (2008) Lanthanide centered covalently bonded hybrids through sulfide linkage: molecular assembly, physical characterization and photoluminescence. Inorg Chem 47:5601
24. Liu JL, Yan B (2008) Lanthanide (Eu^{3+}, Tb^{3+}) centered hybrid materials using modified Functional bridge chemical bonded with silica: molecular design, physical characterization and photophysical properties. J Phys Chem B 112:10898
25. Zhao LM, Yan B (2006) Luminescent enhancement effect in heterometallic terbium-lanthanum hybrid molecular materials obtained by functional bridge grafting to silica network. J Lumin 118:317
26. Wang FF, Yan B (2007) Co-luminescence effect of heterometallic terbium–gadolinium hybrid molecular materials constructed by covalent grafting. J Luminescence 17:418
27. Wang FF, Yan B (2008) Intramolecular energy transfer and luminescence enhancement effect in inert RE^{3+}-Eu^{3+} (Tb^{3+}) (RE = La, Y, Gd) co-fabricated organic-inorganic hybrid materials by covalent grafting. J Photochem Photobiol A Chem 194:238
28. Sarwar MI, Ahmad Z (2000) Interphase bonding in organic–inorganic hybrid materials using aminophenyltrimethoxysilane. Euro Polym J 36:89
29. Liu D, Wang ZG (2008) Novel polyaryletherketones bearing pendant carboxyl groups and their rare earth complexes. Part I: Synthesis and characterization. Polymer 49:4960
30. Yan B, Qiao XF (2007) Rare earth/inorganic/organic polymeric hybrid materials: molecular assembly, regular microstructure and photoluminescence. J Phys Chem B 111:12362
31. Qiao XF, Yan B (2009) Hybrid materials of lanthanide centers/functionalized 2-thenoyltrifluoroacetone/silicon–oxygen network/polymeric chain: coordination bonded assembly, physical characterization, and photoluminescence. Inorg Chem 48:4714
32. Hoffmann HS, Staudt PB, Costa TMH, Moro CC, Benvenutti EV (2002) FTIR study of the electronic metal-support interactions on platinum dispersed on silica modified with titania. Surf Interface Anal 33:631
33. Carlors LD, Bermudez VD, Ferreira RAS, Marques L, Assuncao M (1999) Sol-gel derived urea cross-linked organically modified silicates. 2. blue-light emission. Chem Mater 11:581
34. Goncalves MC, Bermudez VD, Ferreira RAS, Carlos LD, Ostrovskii DJ, Rocha J (2004) Optically functional di-urethanesil nanohybrids containing Eu^{3+} ions. Chem Mater 16:2530
35. Guo XM, Wang XM, Zhang HJ, Fu LS, Guo HD, Yu JB, Carlos LD, Yang KY (2008) Preparation and luminescence properties of covalent linking of luminescent ternary europium complexes on periodic mesoporous organosilica. Microp Mesop Mater 116:28
36. Zhang WH, Lu XB, Xiu JH, Hua ZL, Zhang LX, Robertson M, Shi JL, Yan DS, Holmes JD (2004) Synthesis and characterization of bifunctionalized ordered mesoporous materials. Adv Funct Mater 14:544
37. Li HH, Inoue S, Machida K, Adachi G (1999) Preparation and luminescence properties of organically modified silicate composite phosphors doped with an europium(III) β-diketonate complex. Chem Mater 11:3171
38. Qiao XF, Yan B (2008) Assembly, characterization, and photoluminescence of hybrids containing europium (III) complexes covalently bonded to inorganic Si–O networks/organic polymers by modified β-diketone. J Phys Chem B 112:14742
39. Zhou RS, Ye L, Ding H, Song JF, Xu XY, Xu JQ Syntheses, structures, luminescence, and magnetism of four 3D lanthanide 5-sulfosalicylates. J Solid State Chem 181: 567
40. Dexter DL (1953) A theory of sensitized luminescence in solids. J Chem Phys 21:836
41. Yan B, Zhang HJ, Ni JZ (1998) Photophysical properties of some binary and ternary complexes of rare earth ions with aminobenzoic acids and 1, 10-phenanthroline. Monafsh Chem 129:151
42. Crosby GA, Whan RE, Alire RM (1961) Intramolecular energy transfer in rare earth chelates-role of the triplet state. J Chem Phys 34:743